Methodology for the Immobilization of Enzymes onto Mesoporous Materials

Sarah Hudson,* Edmond Magner,* Jakki Cooney, and B. Kieran Hodnett*

Materials and Surface Science Institute and Department of Chemical and Environmental Sciences, University of Limerick, Limerick, Ireland

Received: April 22, 2005; In Final Form: July 25, 2005

Cytochrome *c* and xylanase were adsorbed onto two mesoporous materials, SBA-15 (a pure silicate) and MSE (an organosilicate), with very similar physical properties but differing chemical compositions. A methodical order was developed whereby the influences of surface area, pore size, extent of order, particle size, surface potentials, isoelectric points, pH, and ionic strength on immobilization were explored. In silico studies of cytochrome *c* and xylanase were conducted before any immobilization experiments were carried out in order to select compatible materials and probe the interactions between the adsorbents and the mesoporous silicates. The stabilities of the mesoporous materials at different pH values and their isoelectric points and zeta potentials were determined. Electrostatic attraction dominated protein interactions with SBA-15, while weaker hydrophobic interactions are more prominent with MSE for both cytochrome *c* and xylanase. The ability of the immobilized protein/enzyme to withstand leaching was measured, and activity tests and thermostability experiments were conducted. Cytochrome *c* immobilized onto SBA-15 showed resistance to leaching and an enhanced activity compared to free protein. The immobilized cytochrome *c* was shown to have higher intrinsic activity but lower thermostability than free cytochrome *c*. From an extensive characterization of the surface properties of the silicates and proteins, we describe a systematic methodology for the adsorption of proteins onto mesoporous silicates. This approach can be utilized in the design of a solid support for any protein.

Introduction

In the past decade much work has been undertaken in the synthesis of mesoporous silicates (MPS) and in the immobilization of enzymes onto these supports. In 1992, the Mobil research group[1] discovered the M41S family of mesoporous silicates which had a narrow pore size distribution, amorphous silica surfaces, and pore sizes in the range of 20−300 Å. These new regular repeating mesoporous structures offered the possibility of adsorbing or entrapping large molecules within their pores. Since their development, these materials have given life to a whole new area of catalytic research. It was anticipated that MPS would provide a sheltered protected environment in which reactions with selected substrates could proceed. Since their initial discovery, mesoporous structures have been synthesized using cationic,[1] neutral,[2] and block copolymer[3] surfactants, have had organic functional groups[4,5] and metals[6] located within their framework or grafted[7] onto their surface, and have been used as a scaffold to develop mesoporous carbon materials.[8]

Enzymes catalyze reactions with high specificity. Unfortunately, they are not always suited to industrial or medical applications. They are often unstable and show low activity in organic solvents or at high temperatures. Denaturation of the enzyme, which destroys its catalytic activity, can often be induced by pH or mechanical or thermal treatment. In industrial processes, the enzyme is often denatured during its removal from the reaction mixture. This is uneconomical as active enzyme is lost. These disadvantages of enzymes can be overcome by immobilization of the enzyme onto a solid structure.[9−17] With increased mechanical stability and potential for recycling, the advantages of enzymes in catalyzing specific reactions under mild conditions could be harnessed via immobilization.

In 1996, Diaz and Balkus[10] first attempted to immobilize enzymes onto mesoporous MCM-41. Since then, research groups[11−17] have established that many factors have a strong influence on the enzyme loading and on the activity of the resultant biocatalyst, including the relative sizes of the mesopores and the enzyme, surface area, pore size distribution, mesopore volume, particle size, ionic strength, isoelectric point, and surface characteristics of both the support and the enzyme. However, there has been no methodical order published which could be followed to evaluate the effect of each variable on the adsorption of a particular enzyme into a particular mesoporous support. The numerous factors mentioned must all be systematically studied in order to understand the immobilization process and to predict which enzymes/proteins will adsorb well while retaining their activity and stability.

These factors, examined in methodical fashion, should result in the best immobilization conditions being found for any given enzyme and support as efficiently as possible. In this study, the adsorption of cytochrome *c* and xylanase onto both SBA-15[3] and MSE[4] were systematically examined according to Scheme 1. Cytochrome *c* has often been studied in immobilization studies,[11,12] with many of the factors governing its immobilization known. Thus, it represents an appropriate protein standard to use when trying to understand and create a systematic method, examining a broad range of factors influencing immobilization. Xylanase was chosen as a test case enzyme. It is used widely in paper production, but it is susceptible to heat denaturation above ∼60 °C.[18,19] Aside from contributing to the general understanding of immobilization techniques,

* To whom correspondence should be addressed. Phone: +353-61-202629. Fax: +353-61-202568. E-mail: sarah.hudson@ul.ie (S.H.); edmond.magner@ul.ie (E.M.); kieran.hodnett@ul.ie (B.K.H.).

10.1021/jp052102n CCC: $30.25
Published on Web 09/24/2005

SCHEME 1: Generation of an Immobilized Enzyme/Protein Biocatalyst

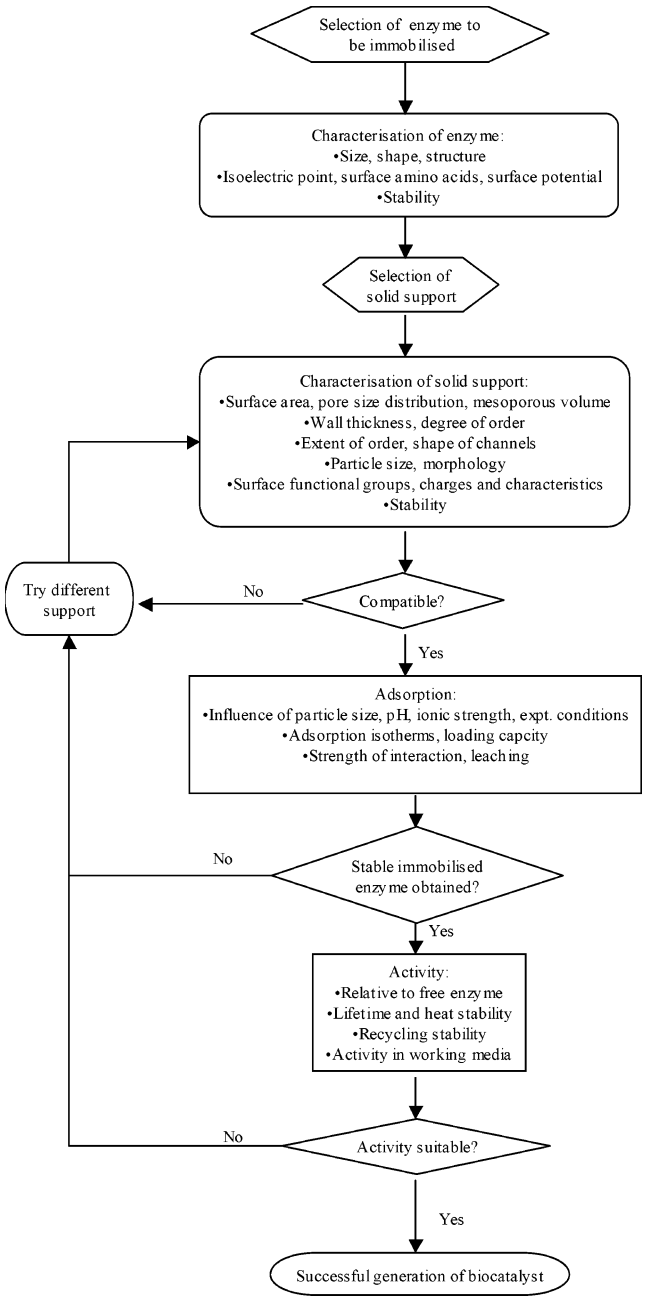

immobilization inside the pores may result in the increased thermostability of xylanase.

This study utilized two previously characterized mesoporous supports, SBA-15[3] and MSE.[4] Both materials were synthesized with the pluronic surfactant, P123. MSE is a periodic mesoporous organosilane (PMO), while SBA-15 is a pure silica material. PMOs have a regular repeating organic moiety within their ordered framework and are prepared from the condensation of bridged alkoxysilicates in the presence of a surfactant. MSE consists of SiO_2 units with $-CH_2CH_2-$ groups interspersed periodically (Figure 1). MSE and SBA-15 were found to have very similar physical properties but different chemical compositions. These differences resulted in very different adsorption behavior with cytochrome *c* and, to a lesser extent, with xylanase. Vinu et al.[13] recently suggested that mesoporous carbon was a much better adsorbent for biomaterials than mesoporous silicates due to its higher water stability, a very

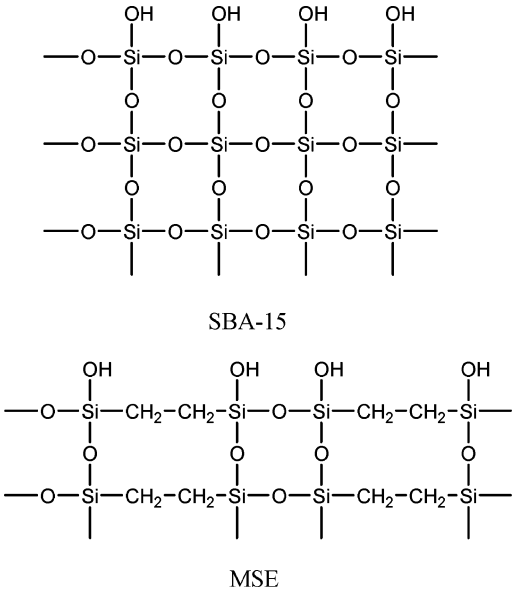

Figure 1. Composition and surface characteristics of SBA-15 and MSE.

desirable property, and neutral surfaces. However, lysozyme was easily leached from the carbon adsorbents when washed with the immobilization buffer. Similarly, we have shown that while adsorption isotherms may exhibit Langmuir-type behavior (cytochrome *c* adsorbing onto MSE), this does not necessarily result in the formation of a stable immobilized enzyme. Ultimately, a successful immobilized enzyme biocatalyst must be fixed to its support in such a way as to withstand additions of fresh buffer or solutions and yet retain its activity. The balance between maintained activity, high loading, and negligible leaching from the support has often proved elusive.[10,13,14] Extensive characterization of a support is necessary in order to predict its viability as a good adsorbent for a particular enzyme. In this paper, the influence of surface potentials, isoelectric points, pH, and ionic strength on the immobilization of cytochrome *c* and xylanase into materials with very similar physicochemical characteristics is explored. The use of Scheme 1 as a guide in the development of immobilized enzyme biocatalysts should result in the generation of a library of well-characterized enzymes and supports which can be matched to each other. The stability and activity of the resultant biocatalyst can then be ascertained.

Experimental Section

Materials. Pluronic P123 ($EO_{20}PO_{70}EO_{20}$) was obtained from BASF. Tetraethoxysilane (TEOS, 98%), 1,2-bis(trimethoxysilyl)ethane (BTMSE, 96%), 2-cyanoethyltriethoxysilane (CEOS), sodium hydroxide, horse heart cytochrome *c* (90%), cetyltrimethylammonium bromide (CTAB), 2,2′-azino bis (3-ethylbenzthiazoline-6-sulfonic acid) (ABTS), trizma base (99.9%), acetic acid, sodium acetate, potassium hydrogen phosphate, potassium dihydrogen phosphate, sodium hydrogen carbonate, and sodium carbonate were all obtained from Sigma-Aldrich. endo-1,4-β-Xylanase II (XYNII of *Trichoderma sp.*) was obtained from Hampton Research.

Synthesis and Characterization of SBA-15, MSE, and MCM-41/28. SBA-15,[3] MSE,[4] and MCM-41/28[15] were prepared using published protocols. For SBA-15, the triblock polymer, Pluronic P123, was used as the templating agent and tetraethoxysilane as the silica source in an acidic medium[3]. For MSE, P123 was used as the templating agent and 1,2-bis-

(trimethoxysilyl)ethane (BTMSE) as the silica source in a less acidic medium.[4] After synthesis, the P123 template was removed by Soxhlet extraction (5 h, repeated twice) using ethanol. For MCM-41/28, CTAB was used as the surfactant in a basic medium and was removed by calcination after synthesis.

Nitrogen gas adsorption/desorption isotherms were measured at 77 K using a Micromeritics ASAP 2010 system. Samples were pretreated by heating under vacuum at 348 K for 12 h. The surface area was measured using the Brunauer−Emmett−Teller (BET) method.[20] The pore size data were analyzed by the thermodynamic-based Barrett−Joyner−Halenda (BJH) method[21] on the adsorption and desorption branches of the N_2 isotherm. Particle size was measured using a Malvern 2000 particle size analyzer. Samples were pretreated by sonication for 15 min and stirring in aqueous solution at room temperature for 24 h. Transmission electron microscopy was conducted using a JEOL JEM-2011 electron microscope operated at an accelerating voltage of 200 kV. The powder was placed directly on a Formbar-backed carbon-coated copper grid. Scanning electron microscopy was conducted using a JEOL JSM 840 with a Princeton gamma technology energy dispersive spectrometer. Samples were dried and ground before SEM analysis. Powder X-ray diffraction data was obtained on a Philips X'pert diffractometer using Ni filtered Cu Kα radiation with $\lambda = 1.54$ Å. Samples were analyzed from 0.3° to 70° 2θ. Isoelectric points were measured using a Malvern Zetasizer 3000HSA. Samples were made up in 18.2 MΩ deionized water (Elgastat) at a concentration of ∼0.5 mg/mL and were sonicated for 15 min before zeta potential measurements were taken. The pH of the solution was manually adjusted by the addition of 0.1 M HCL or NaOH to ca. 10−15 mL of the suspension before its zeta potential was measured.

Adsorption of Protein to Mesoporous Supports. Protein concentrations in solution were calculated from their absorbances at 409 nm ($\epsilon = 100\,000$ M^{-1} cm^{-1})[24] and at 278 nm ($\epsilon = 57\,059$ M^{-1} cm^{-1})[25] for cytochrome *c* and xylanase, respectively. The initial protein concentration was established by mixing 0.5 mL of buffer and 0.5 mL of the protein solution, followed by centrifugation and measuring the UV−vis absorbance of the supernatant at the appropriate wavelength. A suspension of mesoporous support in the relevant buffer at a concentration of 2 mg/mL was sonicated for 15 min and stirred for ∼30 min on a magnetic stirrer to create a dispersed solution. Equivalent volumes of the protein solution and the suspension were then mixed together and incubated as outlined below. The protein loading at any particular time was calculated by taking 1 mL samples from the reaction vessel, centrifuging, measuring the protein concentration of the supernatant, and taking this value from the initial concentration. Experiments with stirring were carried out with a magnetic stirrer in a covered beaker at room temperature. Experiments with shaking were carried out in a New Brunswick Scientific C24 incubator shaker (120 rpm, 25 °C). Xylanase adsorption experiments were conducted in a similar manner. To generate the adsorption isotherms, different initial protein concentrations were used. To examine the effect of ionic strength on adsorption, the ionic strength of the solution was varied from 0.01 to 2 M by the addition of NaCl. Leaching experiments were carried out by washing ∼2 mg of loaded material with a range of buffers. The normal regime involved 3 washes with the immobilization buffer, followed by 3 washes with a buffer of different pH value, and finally 3 washes with a buffer of higher ionic strength.

Activity Assays. The activity assay used to measure cytochrome *c* activity was the oxidation of ABTS, which was followed spectrophotometrically at 405 nm ($\epsilon_m = 36\,800$ M^{-1} cm^{-1}).[11] Assay mixtures for immobilized protein contained silicate (2 mg, 0.5−30 μmol/g), ABTS (0.54 mM), and H_2O_2 (7.5 mM) in a 1 mL reaction vessel. Assay mixtures for the free protein contained cytochrome *c* (1−60 μM), ABTS (0.54 mM), and H_2O_2 (7.5 mM). All reagents were in 25 mM potassium phosphate buffer at pH 6.5.[11] Assays were performed at room temperature.

Thermostability. Thermostability experiments were conducted by heating a solution of free cytochrome *c* and a suspension of cytochrome *c*/SBA-15 in sealed containers in an oven at the desired temperature for the desired amount of time. When removed for activity tests, the solutions were allowed to cool to room temperature, aliquots were removed and the containers were returned to the oven. The cytochrome *c*/SBA-15 suspension was stirred to ensure a uniform suspension when aliquots were removed. All activity assays were conducted at room temperature.

Results and Discussion

Characterization of Protein. Using the protein atomic coordinates 1HRC (cytochrome *c*) and 1ENX (xylanase) from the Protein Data Bank (PDB), images of oxidized horse heart cytochrome *c* and endo-1,4-β-xylanase from *Trichoderma reesei* were reconstructed using the software packages PyMOL[22] and DeepView.[23] Cytochrome *c* contains approximately 40% α-helix[24] while the remainder consists of extended coils. Xylanase, on the other hand, consists of two antiparallel β-sheets, which are packed against each other. The β-sheet structure is twisted forming a large cleft on one side of the molecule.[25] With the use of the DeepView and PyMOL software packages and repeated rotations of the protein/enzyme molecules, the average dimensions of cytochrome *c* were found to be 30 Å at the narrowest and 40 Å at the widest. Xylanase was found to be approximately 40 Å wide in all directions. These measurements are consistent with the published unit cell parameters for cytochrome *c* and xylanase, 58.34 Å × 58.34 Å × 41.83 Å (spherical diameter of ∼40 Å)[27] and 81.6 Å × 60 Å × 38.3 Å (for two molecules),[25b] respectively.

Cytochrome *c* and xylanase both have high isoelectric points (pI), ∼10.7[24] and ∼9.0,[25] respectively. The very basic pI of cytochrome *c* is a result of the high content of basic amino acids (19 K, 2 R, and 3 H residues) when compared to that of the acidic residues (9 E and 3 D). Xylanase contains 13 basic amino acids (4 K, 6 R, and 3 H) and 8 acidic amino acids (4 E and 4 D). In comparing the surface distribution of amino acids in cytochrome *c* and xylanase, it is clear that xylanase contains a much lower density of basic amino acids close to its surface (and throughout the entire molecule). On comparison of the two images (through 360°), the surface of xylanase is composed of more polar and nonpolar residues than that of cytochrome *c* (Figure 2, images constructed in PyMOL[22]).

With the use of the GRASP[30] modeling program, the Poisson−Boltzmann surface electrostatic potentials of cytochrome *c* and xylanase were computed, based on PDB coordinates. A positive surface potential is shown in blue and negative in red in Figure 2. The electrostatic surface of cytochrome *c* consisted of large patches of positive charge with a few smaller patches of negative charge. Xylanase, on the other hand, contains a strongly negatively charged region around the active site but has no other distinct areas of charge on its surface. These theoretical calculations support the conclusion drawn from the discussion on the amino acid content above, namely, that cytochrome *c* would have a much greater positive charge

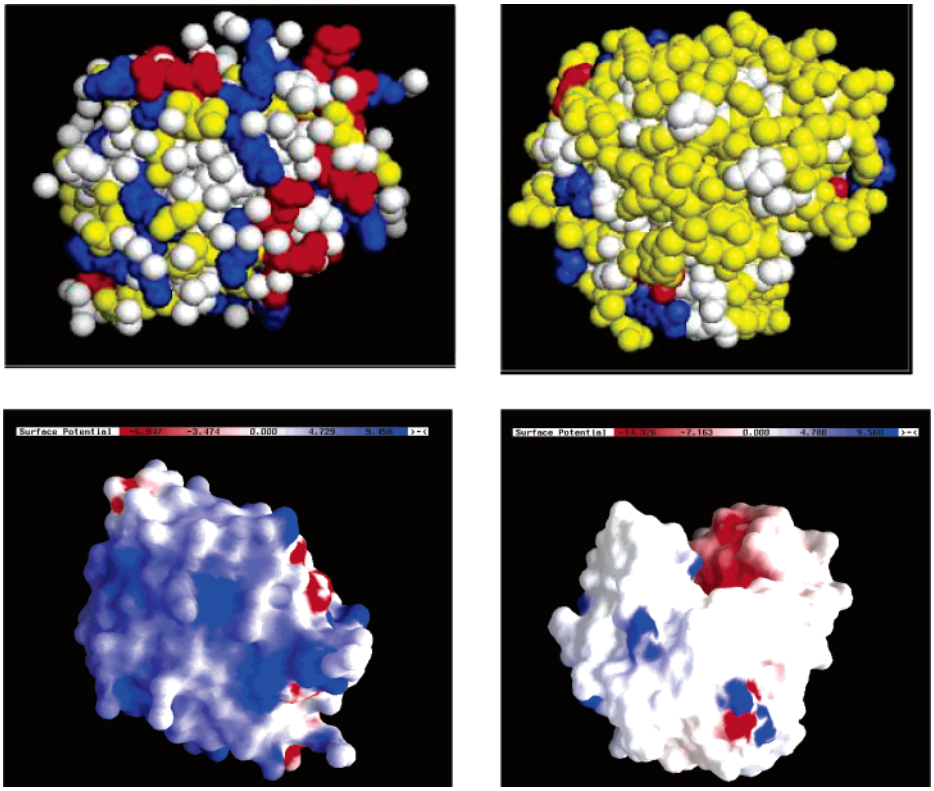

Figure 2. Top: Amino acid composition of cytochrome *c* (left) and xylanase (right) (blue, basic amino acids; red, acidic amino acids; yellow, polar amino acids; white, nonpolar amino acids). Bottom: Poisson−Boltzmann electrostatic potentials of cytochrome *c* and xylanase, calculated by GRASP.[30]

associated with its surface than xylanase. In silico characterization of the electrostatic surface potential of the two biomaterials indicates that cytochrome *c* should interact more strongly with a negatively charged surface, while xylanase may have more affinity for a hydrophobic or polar surface.

Before any adsorption experiments could be carried out, the stability of the enzyme/protein under the experimental conditions chosen for the adsorption processes was checked. The buffers used with cytochrome *c* were 10 mM acetate pH 4.0, 10 mM and 25 mM phosphate pH 7.0, and 10 mM carbonate pH 10. For xylanase, 10 mM phosphate pH 7.0 and 10 mM Tris−HCl pH 8.9 buffers were used. Cytochrome *c* showed no loss in solubility with stirring or shaking in its four buffers at 25 °C over 24 h at all concentration ranges. Xylanase was found to show no loss in solubility when the solution was not stirred at room temperature over 24 h, but when stirred, a decrease in concentration of soluble enzyme was observed after ∼10 h, which decreased further with time. When the shaker was used, xylanase remained in solution at room temperature for at least 24 h. A number of immobilization procedures for the adsorption of enzymes onto mesoporous supports have been reported, but the stability of the enzymes under the experimental conditions used must be examined. Stirring has often been used as a means of agitating the reaction mixture[10,14,16] but may lead to aggregation and precipitation of the protein. In this work, care was taken not to assign a decrease in concentration of a xylanase solution to a loading onto a support. Appropriate controls in all adsorption experiments involving both enzymes were used.

Characterization of Support. Suitable adsorbents had to have pore sizes of 30 Å or greater if the internal surface area of the supports is to be accessible to cytochrome *c* and greater than 40 Å for xylanase. SBA-15 and MSE were used, since both have high surface areas and pore diameters large enough to allow cytochrome *c* and xylanase to access the internal surface. Cytochrome *c* should interact strongly with a negatively charged surface. Xylanase may undergo similar electrostatic interactions with a negative surface, but other forces of attraction with a more polar or hydrophobic surface may also occur. It is important to fully characterize the adsorbents if the nature of the interaction between the biomaterial and solid support is to be described. The physical properties of the solid support also have a large influence on immobilization. SBA-15 and MSE differ little in their physical properties but significantly in their chemical compositions.

TABLE 1: Physicochemical Properties of SBA-15 and MSE Obtained from Nitrogen Adsorption Analysis

	surface area (m^2/g)	C_{BET}	d_{BJH} (Å)[a]	d_{BJH} (Å)[b]	total pore vol (cm^3/g)	mesopore pore vol (cm^3/g)
SBA-15	1007	107	63	78	1.15[c]	0.46[c]
MSE	1223	106	62	77	1.32[c]	0.51[c]

[a] Calculated from the desorption branch of the nitrogen isotherm. [b] Calculated from the adsorption branch of the nitrogen isotherm. [c] Volume of liquid nitrogen at STP.

The physicochemical properties of SBA-15 and MSE, in agreement with published data,[3,4] are shown in Table 1. Surface area (BET theory), average pore diameter, and total pore volume were calculated using nitrogen adsorption/desorption analysis (Figure 3). Both materials exhibit a type IV adsorption isotherms (Brunauer definition), where the volume of nitrogen adsorbed increases with increasing relative pressure with a sharp rise in adsorption due to capillary condensation in the mesopores. Both materials contain some degree of microporosity due to the penetration of the framework walls by the hydrophilic poly(ethylene oxide) (PEO) moieties of P123. MSE contains a slightly greater population of micropores than SBA-15 judging by the higher amount of nitrogen adsorbed at low relative pressures. As suggested in the literature,[26] this may arise because

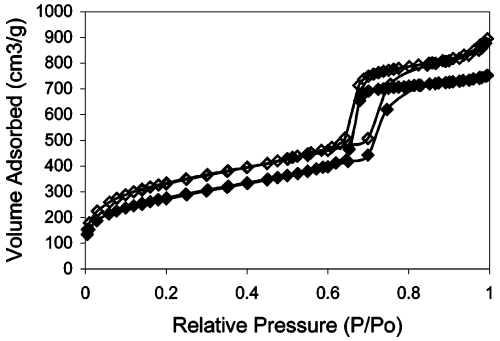

Figure 3. N_2 Adsorption/desorption isotherms for (◆) SBA-15 and (◇) MSE.

TABLE 2: Physicochemical Properties and Positions and *d*-Spacings of Reflection Peaks in Low-Angle XRD Patterns for SBA-15 and MSE

	position $2\theta°$	*d*-spacing (Å)	hkl	pore center−pore center (Å)	wall thickness (Å)[a]
SBA-15	0.9352	95	100	110	32
	1.6019	55	110		
	1.8771	47	200		
MSE	0.7937	111	100	128	51
	1.4067	63	110		
	1.6328	54	200		

[a] Calculated using the pore diameter from the adsorption branch of the N_2 isotherm.

the enhanced hydrophobic walls of MSE may allow the PEO blocks to penetrate deeper into the framework walls and thus generate more microporosity in the final structure. The slight upward curve of the MSE isotherm as the relative pressure approaches 1 also indicates the possible presence of some larger interparticle macro/mesopores. The mesopore volume was calculated from the increment in volume of nitrogen adsorbed in the sharp rise in the adsorption/desorption isotherm. This method underestimates the mesopore volume because it neglects to take into account the volume of nitrogen in the initial monolayer adsorbed onto the surface of the mesopores before capillary condensation occurs.

The d_{100}-spacing, the pore center to pore center distance, and the wall thickness of these materials were calculated from the low-angle XRD patterns, and the pore diameters were obtained using BJH theory. Both materials demonstrated a 2-dimensional hexagonal pattern with the Miller indices shown in Table 2. Wall thickness was calculated as the difference between pore center to pore center length, as measured by XRD, and the average pore diameter, as measured by porosimetry using the adsorption branch of the isotherm. Transmission electron microscopy (TEM) can be used to see the extent of order in these materials and also the shape and regularity of the channels. Care must be taken to note the focusing conditions and magnification under which the image is taken. Images of SBA-15 and MSE in the underfocused mode are shown in Figure 4. Note that these ordered channels were seen in nearly every particle examined. The image contrast of the mesoporous particle originates from phase contrast. However, the location of these fringes is not necessarily coincident with the exact projected location of the boundary between the silica matrix and the pore, and thus, exact measurements of pore sizes and wall thickness cannot be taken from these images.

The particle sizes of SBA-15 and MSE were measured using light-scattering analysis and were greatly reduced when sonicated and/or stirred vigorously, Table 3. Sonication for 15 min

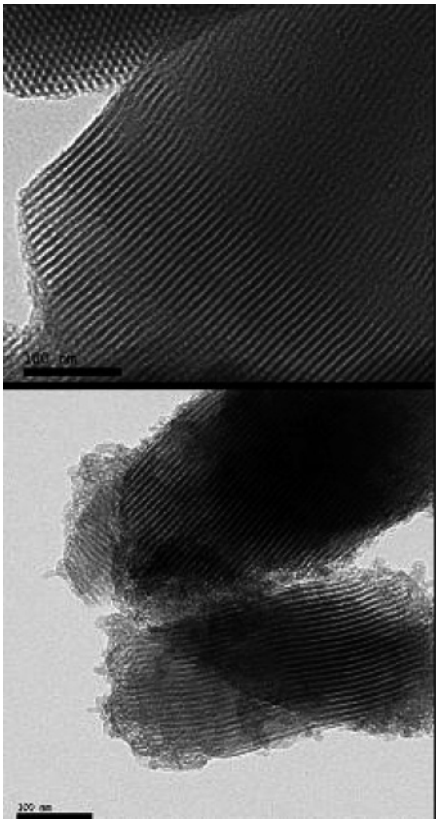

Figure 4. TEM images of SBA-15 (top, scale bar 100 nm) and MSE (bottom, scale bar 100 nm) taken in the underfocused mode.

TABLE 3: Average Particle Size of SBA-15 and MSE

	post-Soxhlet extraction (μm)	post sonication (μm)
SBA-15	300	20
MSE	220	16

of both SBA-15 and MSE (in the buffer to be used in adsorption experiment) reduced the particle size to 20 μm and 16 μm, respectively. XRD analysis and nitrogen adsorption analysis showed that sonication and stirring does not alter the fundamental hexagonal ordered channel structure of the material (see below). The morphology of SBA-15 and MSE particles was examined using scanning electron microscopy. The corresponding images are shown in Figure 5. Both materials consisted of cylindrical rods. The links in the MSE chains seem slightly shorter and are connected in more ordered, straighter chains than those in SBA-15. The shapes of the SBA-15 links are slightly more oval and slightly bigger than those in MSE. The structure of the MSE particles is more fiber-like than the SBA-15 particles.

In agreement with previously published work,[3,4] SBA-15 is a pure silica material consisting of SiO_2 units with Si−OH hydroxyl groups on the surface, while MSE consists of SiO_2 units with $-CH_2CH_2-$ groups interspersed periodically. This results in a much lower density of Si−OH groups on the surface of the support (Figure 1). The $-CH_2CH_2-$ groups would be expected to add some hydrophobic character to the mesoporous support. This would result in weaker electrostatic-type interactions with an adsorbate than SBA-15 but could enhance hydrophobic interactions. FTIR analysis confirmed the presence of the ethylene groups in the framework of MSE as well as the removal of the template by Soxhlet extraction to negligible amounts from both SBA-15 and MSE.[26,28] Due to the presence of these small amounts of residual surfactant, CHN analysis,

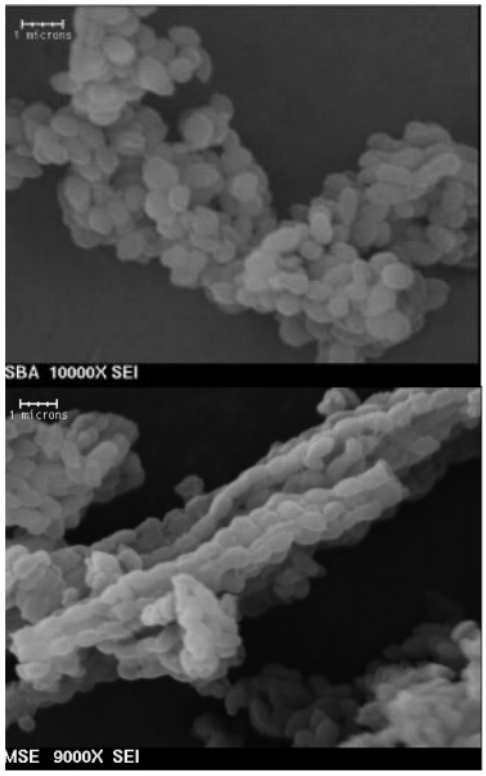

Figure 5. SEM images of SBA-15 (top) and MSE (bottom) particles (scale bar 1 μm).

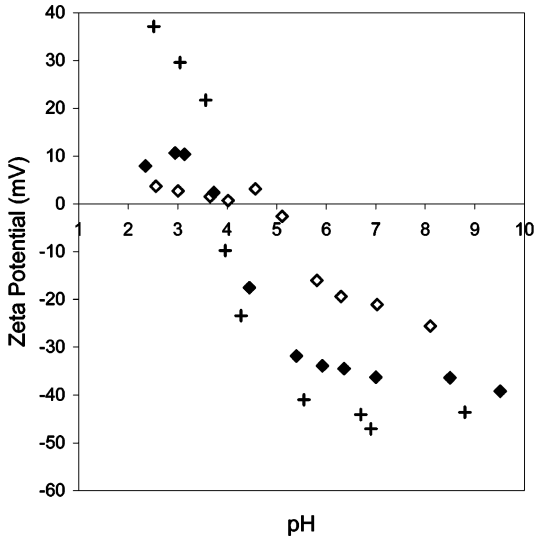

Figure 6. Zeta potential vs pH plot for (◆) SBA-15, (◇) MSE, and (+) MCM-41/28 suspensions.

which can quantify the amount of functional groups present, was not applicable in the case of MSE.

While the isoelectric point of the enzyme has often been considered when undertaking adsorption studies, the isoelectric point of the silica support is often assumed to be in the region of 2.[12] We previously reported[15] the zeta potential of mesoporous silicates to be in the range 2.8 to 3.7). In this study the zeta potential of MPS was determined as a function of pH (Figure 6). The pI of SBA-15 was found to be $\sim 3.7 \pm 0.3$, and the pI of MSE was $\sim 4.8 \pm 0.3$. At a pH of 7−10, both materials will be negatively charged. The magnitude of this negative charge changes as the pH increases. SBA-15 has a larger negative charge than MSE at pH values in the range of 5.0−8.5. At pH values above 8.5, the pH value is unstable due to some decomposition of the materials. The thick walls of SBA-15 and MSE mean that they still retain their structure and order at these high pH values (see the discussion on the stability of supports), but a steady pH value was difficult to obtain.

The plot of zeta potential versus pH for MCM-41/28 has been added in for comparison purposes. MCM-41/28 is synthesized with a cationic surfactant but has a similar isoelectric point to SBA-15, ~3.7. However, the magnitude of its zeta potential both at low and high pH values is much larger than for the materials synthesized with the nonionic surfactant, P123. This observation is supported by published literature where SBA-15 was suggested to have less negative potential on its surface compared to materials synthesized with cationic surfactants.[16] Takahashi et al.[16] illustrated this by studying the adsorption of cationic and anionic pigments onto SBA-15, FSM, and MCM-type materials. SBA-15 was found to adsorb the lowest amount of cationic pigment, while all three adsorbed similar amounts of anionic pigment. The larger pore sizes of SBA-15 compared to those of many MCM-type materials could compensate for its lower electrostatic potential, with less pore blocking, larger pore volumes available, etc. These results indicate that the magnitude of charge on the mesoporous silica surface, at pH values away from the isoelectric point, depends on the surfactant used and the chemical composition of the final structure.

The stability of SBA-15 and MSE in a range of buffers was determined. The XRD patterns show that after sonication for 15 min and stirring for 24 h in buffer, no significant changes in the structure of SBA-15 or MSE were observed and no reduction in intensities was observed. Thus, SBA-15 and MSE appear to retain their hexagonal ordered structure under the experimental conditions in this study. There was a small loss in the resolution of the third peak at 1.833° (2θ) for SBA-15 stirred in buffer at pH 10, but this did not appear to result in a significant change in structure. SBA-15 and MSE samples were dried in a vacuum oven at 120 °C after sonication and stirring in the buffer solutions before undergoing nitrogen adsorption analysis again. The results are shown in Table 4. These indicate a large reduction (up to 56%) in the surface area of SBA-15. This was most likely as a result of adsorption of the salt ions onto the surface of the support—it was found that the surface area was restored to its original value after two washings with the deionized water, Table 5. MSE underwent a smaller loss in surface area (up to 38%) due to the adsorption of the salt ions. XRD analysis showed that the *d*-spacing did not change significantly. A small change in the pore diameter was observed. While the overall total pore volume was significantly reduced (again, probably due to adsorption of salt ions), the mesoporous volume remained close to its original value. For comparison purposes, the stability of MCM-41/28 at pH 10 was studied. After sonication and stirring, the MCM-41/28 had lost much of its structure, illustrated by changes in the XRD patterns and nitrogen adsorption analysis (note the large drop in mesopore volume). Overall, despite sonication and stirring in a solution at pH 10, both SBA-15 and MSE retained their hexagonal ordered structures and narrow mesopore size distributions.

Adsorption Studies. Having fully characterized cytochrome *c*, xylanase, SBA-15, and MSE, it would seem that cytochrome *c* and SBA-15 would be reasonably compatible, with electrostatic interactions being the driving force for immobilization. While xylanase may also adsorb onto SBA-15, its less positive predicted surface potential may result in weaker electrostatic interactions. MSE has more hydrophobic character than SBA-15 and may interact with any nonpolar patches on the surface of the proteins. Cytochrome *c* and xylanase were adsorbed onto

TABLE 4: Physicochemical Properties of SBA-15, MSE, and MCM-41/28 after Sonication and Stirring in Buffers (i) 10 mM Citric Acid/Sodium Citrate pH 4, (ii) 10 mM KH_2PO_4/K_2HPO_4 pH 7, (iii) 10 mM $NaHCO_3/Na_2CO_3$ pH 10, and (iv) 10 mM Tris−HCl pH 8.9

material	surface area (m^2/g)	$d_{BJH,desorp}$ (Å)	$d_{BJH,adsorp}$ (Å)	total pore vol (cm^3/g)	mesopore pore vol (cm^3/g)	wall thickness (Å)[a]
SBA-15	1007	63	78	1.15	0.46	32
(i) pH 4	555	39	64	0.36	0.09	
(ii) pH 7	470	60	76	0.72	0.36	34
(iii) pH 8.9	529	61	76	0.80	0.42	34
(iv) pH 10	444	61	76	0.83	0.46	38
MSE	1223	62	77	1.32	0.51	51
(i) pH 4	899	59	75	0.9	0.36	
(ii) pH 7	851	60	77	1.05	0.43	50
(iii) pH 8.9	841	60	77	0.98	0.38	40
(iv) pH 10	754	59	77	0.98	0.38	46
MCM-41/28	1126	28	30	0.92	0.32	16
(i) pH 10	655	(21)[b]	24	0.51	0.05	

[a] Calculated using the pore diameter from the adsorption branch of the N_2 isotherm. [b] No peak—the increase at 2.1 nm corresponds to micropores.

TABLE 5: Changes in Surface Area of SBA-15 Due to Salt Ion Adsorption and Washing with Water

	surface area (m^2/g)	C_{BET}
original SBA-15	893	153
SBA-15 pH 7	670	95
SBA-15 pH 7 washed	839	91

both supports for illustrative purposes, in an attempt to qualify the type of interaction between each biomaterial and support.

It has been shown previously that the particle size of powder samples has a strong influence on the adsorption kinetics of large biomolecules into mesoporous silicates.[17] The smaller the particles, the faster the cytochrome *c* can adsorb onto SBA-15 (Figure S3 in the Supporting Information). Fast immobilization procedures minimize the risk of enzyme denaturation during the adsorption process. In general, the smaller the particle size, the faster the immobilization. Pretreatment by stirring or sonication does not change the fundamental structure, length, or number of pore openings of the SBA-15 material, and thus, when equilibrium is reached, the final loading capacity of the material has not increased.

Adsorption experiments were carried out for cytochrome *c* onto SBA-15 (Figure 7A) in buffers at different pH values. The influence of pH on the rate of the adsorption process and on the magnitude of the loadings on SBA-15 was examined. The isoelectric point of SBA-15 is ~3.7 ± 0.3, while that of cytochrome *c* is ~10.7.[24] In pH 10 with an initial concentration of 22 μM, all of the cytochrome *c* present was adsorbed. At pH 10, SBA-15 is highly negatively charged while cytochrome *c* will have close to an overall neutral charge. Close to the isoelectric point, cytochrome *c* molecules will exhibit less repulsion between themselves and thus will be able to pack closer together onto the surface of the adsorbent. Close to the surface of SBA-15, the pH at the interface may differ from that of the bulk solution due to the highly negatively charged silica surface. It has been suggested in the literature that the pH at the interface may be as much as two units lower than that of the bulk solution.[29] This would explain why the interaction between the cytochrome *c* molecules and the surface of SBA-15 is still reasonably strong. At pH 7, with an initial cytochrome *c* concentration of 24 μM, equilibrium took a little longer to attain compared to that at pH 10. A final loading of ~19 μmol/g was obtained. At a pH of 7, SBA-15 will have a negative surface charge while cytochrome *c* has an overall positive charge. Each cytochrome *c* molecule will occupy more space at pH 7 than at pH 10 on the surface as it repels neighboring cytochrome *c* molecules. The longer time necessary to reach equilibrium at pH 7 is most likely due to the repulsion between cytochrome *c* molecules. In pH 4 buffer, the cytochrome *c* molecules will

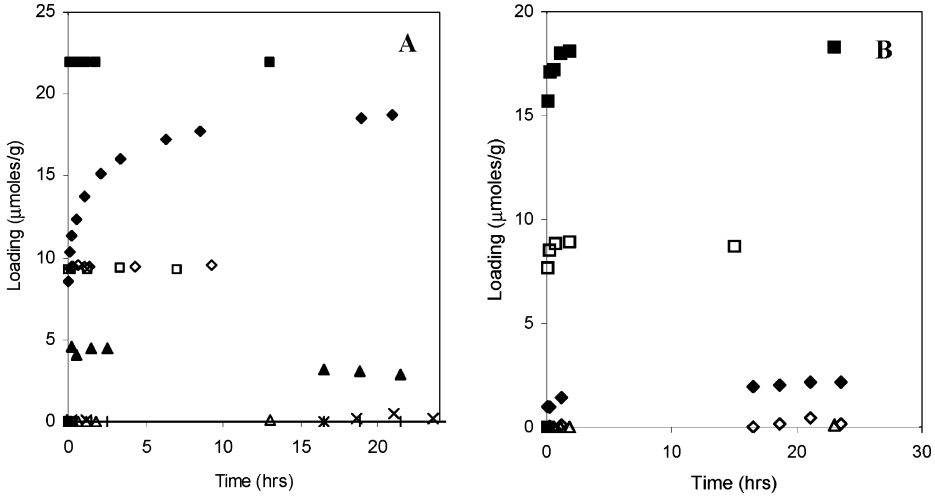

Figure 7. Adsorption of cytochrome *c* at different initial concentrations with stirring at 25 °C in 10 mM sodium acetate−acetic acid, potassium phosphate buffer or sodium carbonate buffer onto SBA-15 and MSE. (A) SBA-15: (▲) pH 4, 19.6 μM; (◇) pH 7, 9.6 μM; (◆) pH 7, 24 μM; (□) pH 10, 9.4 μM; (■) pH 10, 22 μM; with controls (+) pH 4, 19.6 μM; (×) pH 7, 11 μM; (Δ) pH 10, 22 μM. (B) MSE: (◆) pH 7, 11 μM; (□) pH 10, 9.3 μM; (■) pH 10, 22 μM; with controls (◇) pH 7, 11 μM; (Δ) pH 10, 22 μM.

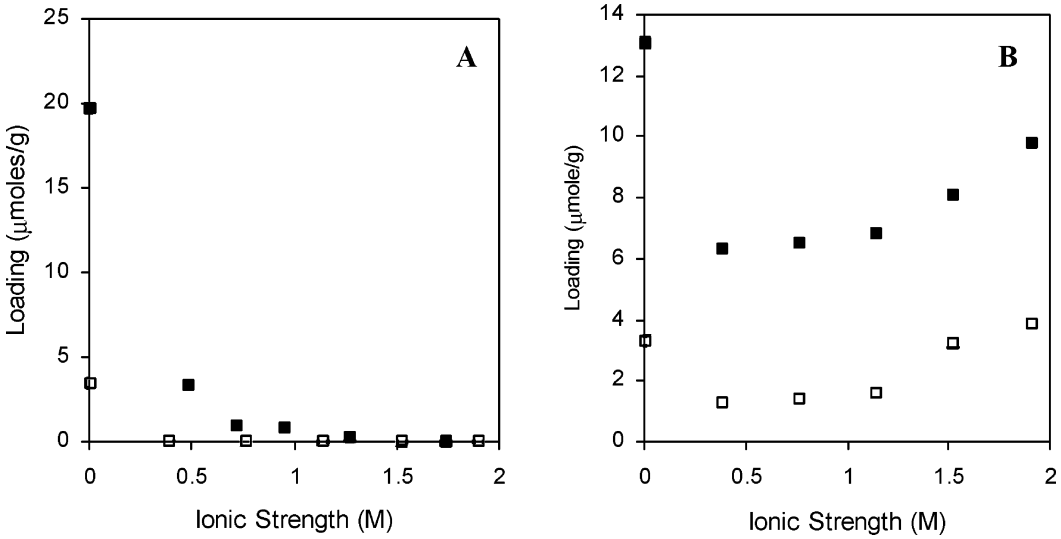

Figure 8. Adsorption onto SBA-15 and MSE with varying ionic strength. (A) SBA-15: (■) cytochrome *c* pH 7, 24.4 μM; (□) xylanase pH 8.6, 12.9 μM. (B) MSE: (■) cytochrome *c* pH 8.6, 22.75 μM; (□) xylanase pH 8.6, 24.3 μM.

have a high positive surface charge, hence each cytochrome *c* molecule will occupy a large space, and repulsions between these molecules will be strong. At the same time, pH 4 is close to the pI of SBA-15, measured to be ~3.8 ± 0.3, and so the surface of SBA-15 will be close to neutral. Most importantly, SBA-15 has been shown to be unstable when sonicated and stirred in pH 4 buffer (Table 4), and it loses its mesoporous structure. These three factors contribute to a low loading of cytochrome *c* onto SBA-15, ~3.0 μmol/g.

Cytochrome *c* showed very little adsorption onto MSE at pH 7—with an initial concentration of 11 μM, a loading of ~3 μmol/g was observed (Figure 7B). However, upon changing the pH of the buffer solution from 7 to 10, with an initial concentration of 9.3 μM, the loading increased to 9.3 μmol/g. This can be attributed to reduced repulsive forces between cytochrome *c* molecules at pH 10 compared to pH 7. When the initial concentration was increased to 22 μM at pH 10, a loading of 18 μmol/g was obtained.

Similar experiments were conducted with xylanase. More xylanase was adsorbed onto SBA-15 at pH 8.9 than 7.3 with stirring at ~4 °C. After 48 h, the xylanase concentration in the supernatant was still falling, but this was due to the xylanase precipitating out of solution rather than any continuous adsorption onto SBA-15. Again, higher loadings of xylanase (~11 μmol/g at pH 8.9 versus ~5 μmol/g at pH 7.3) on SBA-15 were observed at pH values closer to the pI of xylanase, ~9.0. From the enzyme stability experiments, it was deduced that the most stable experimental condition to use was shaking rather than stirring. Much less xylanase was adsorbed onto SBA-15 with shaking, but xylanase is stable in solution under these conditions. Slightly higher amounts of xylanase were adsorbed onto SBA-15 than MSE (~4.5 μmol/g SBA-15, ~3.0 μmol/g MSE, initial concentration of 12.3 μM, pH 8.9).

Despite their similar size and basic isoelectric points, much less xylanase adsorbed onto SBA-15 and MSE than cytochrome *c*. This may be due to less basic amino acid residues residing on the surface of xylanase, reducing the electrostatic interaction. These results support the theoretical surface potentials calculated for cytochrome *c* and xylanase, where cytochrome *c* was shown to have a much stronger, overall positive, surface potential compared to the much weaker surface potential of xylanase with its patches of positive and negative charges (Figure 2). However, reducing the negative charge on the adsorbent surface by using MSE instead of SBA-15 did not greatly change the loading of xylanase. Thus, the adsorption of xylanase cannot rely completely on electrostatic interactions.

Ionic Strength. The effect of ionic strength on adsorption onto the two supports was examined by the addition of NaCl to solutions of cytochrome *c* and xylanase. It was found that increasing the ionic strength of the initial cytochrome *c* and xylanase solutions inhibited adsorption onto SBA-15. There was practically no adsorption of either protein onto SBA-15 when the ionic strength was increased to >0.5 M (Figure 8A). The adsorption of xylanase and cytochrome *c* onto MSE at varying ionic strengths was also examined and more complex behavior was observed (Figure 8B). An initial increase in ionic strength (up to 0.5 M) reduced the loading of both cytochrome *c* and xylanase onto MSE. At higher ionic strength, the loading increased, an increase which cannot arise from a salting out effect as both xylanase and cytochrome *c* were found to be stable in solutions with an ionic strength of 2 M, under the experimental conditions used. These results imply that, for both cytochrome *c* and xylanase, electrostatic interactions dominated the adsorption onto SBA-15 but not onto MSE. Similarly, the reduced surface areas observed with MSE in comparison to those of SBA-15 during the stability studies of the silicates indicated that SBA-15 adsorbed more salt than MSE.

Stability of Immobilized Enzyme. The absolute strength of the interaction between enzyme and support cannot be judged from the adsorption kinetics but can be gauged from the ability of the enzyme to resist removal during washing with different buffers and solutions. Leaching tests of cytochrome *c* from SBA-15 were conducted with 10 mM pH 4, pH 7, and pH 10 buffers and 25 mM pH 7 buffer. Very little leaching (<1%) of cytochrome *c* was observed even at a loading of ~22 μmol/g at pH 10. When cytochrome *c* immobilized on MSE was washed 4 times with the immobilization buffer (pH 10 buffer), ~7% was leached off with each washing. Upon 3 washes with 10 mM pH 7 buffer, ~90% of the cytochrome *c* was removed. Thus, the interaction between cytochrome *c* and the surface of SBA-15 appears to be strong while its interaction with the surface of MSE is much weaker. Very little cytochrome *c* was adsorbed onto MSE at pH 7, indicating that the interaction between MSE and cytochrome *c* is not strong enough to overcome the repulsive forces between the cytochrome *c* molecules. At pH 10, a large increase in the loading value was

observed as the repulsion between cytochrome *c* molecules was reduced. The interaction was still weak as leaching was observed and nearly all the protein was washed off the MSE when the pH of the wash buffer was lowered from pH 10 to pH 7. The maximum amount of cytochrome *c* adsorbed onto SBA-15 under the experimental conditions discussed so far was 22 μmol/g. One cytochrome *c* molecule occupies a volume of 143 nm^3 (from unit cell parameters[27]), thus 22 μmoles will occupy 1.89 cm^3 which is in excess of the mesoporous volume (and total pore volume) in SBA-15. Thus, some of the cytochrome *c* must be found on the external surface of SBA-15.

Leaching tests of xylanase from SBA-15 and MSE with loadings of ~3 μmol/g of xylanase were conducted. When SBA-15 loaded with xylanase was washed with immobilization buffer (pH 8.9), ~30% of the xylanase was removed in the first wash and ~20% (of the loading at that point) removed in each of the two subsequent washings. The wash buffer was then changed to 10 mM pH 10 buffer, and the first wash practically removed all of the remaining xylanase from the SBA-15 (~0.003 μmoles from 2 mg of SBA-15). When xylanase immobilized onto MSE was washed with immobilization buffer, similar results were obtained. When the pH of the wash buffer was increased to pH 10, more xylanase was retained on MSE than it was on SBA-15—but practically all was removed after two washings. The ionic strength experiments suggested that the interaction between xylanase and SBA-15 was electrostatic, but the leaching studies show that it must be a much weaker interaction than between cytochrome *c* and SBA-15. Hydrophobic interactions may dominate in the adsorption of xylanase to MSE, but loadings were low, and the enzyme leached off easily with fresh buffer additions. Higher loadings of cytochrome *c* were observed for MSE, probably with hydrophobic interactions, but again leaching was problematic. Perhaps the hydrophobic character of the support walls needs to be further enhanced to immobilize xylanase more permanently. From Scheme 1, the initial characterization of xylanase showed a low charged surface but with a lot of polar residues residing on the surface, indicating that a more polar support may be more suitable.

Adsorption Isotherms. From the stability tests and adsorption work carried out, the optimum conditions required to generate adsorption isotherms for cytochrome *c* and xylanase on the materials SBA-15 and MSE were deduced. Optimum adsorption isotherms for cytochrome *c* onto SBA-15 and MSE should be carried out in pH 10 buffer, at 25 °C with stirring/shaking, and equilibrium should be reached in less than 5 h. The most suitable immobilization conditions for xylanase onto SBA-15 and MSE require pH 8.9 buffer at 25 °C with shaking. As can be seen from the adsorption isotherm of cytochrome *c* onto SBA-15 (L-type), Figure 9, the maximum loading appears to level off in the region of 35−40 μmol/g. Leaching, of up to 4%, from SBA-15 at these higher loading values was observed when washed with 10 mM pH 7 phosphate in the initial 2−3 washings, but thereafter, leaching was reduced to less than 1% per washing. With shaking and in pH 10 buffer, an adsorption isotherm for cytochrome *c* onto MSE with a maximum loading of ~20 μmol/g was found. Again, the adsorption isotherm appears to be an L-type isotherm, implying a strong interaction between the enzyme molecule and the MSE surface where saturation is quickly attained. Leaching tests indicated that when washed with the immobilization buffer ~7% was leached off in each of three washings. When the pH of the washing buffer was lowered to pH 7, ~40% was leached off in the first wash with ~3% being washed off with every fresh addition of buffer thereafter.

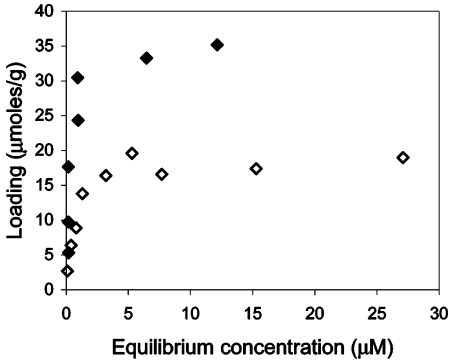

Figure 9. Adsorption isotherms of cytochrome *c* onto SBA-15 and MSE in 10 mM pH 10 with shaking, 120 rpm, at 25 °C for 24 h; (◆) SBA-15, (◇) MSE.

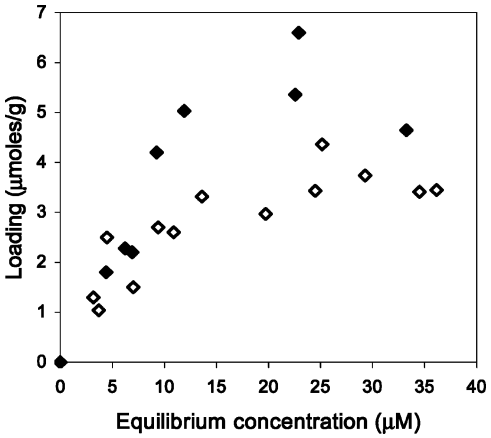

Figure 10. Adsorption isotherm of xylanase onto SBA-15 and MSE in pH 8.9 solution with shaking, 120 rpm, at 25 °C for 24 h; (◆) SBA-15, (◇) MSE.

Adsorption isotherms for xylanase onto SBA-15 and MSE were also conducted, Figure 10. The shapes of the isotherms support the conclusions drawn previously that the interaction between cytochrome *c* and SBA-15 is a much stronger interaction than that between xylanase and SBA-15 and MSE. The adsorption capacity was dependent on the solution concentration of xylanase at lower equilibrium concentrations of xylanase. Eventually, at higher concentrations, saturation of the support with xylanase was observed. Leaching was a significant problem here as each time fresh buffer was added, xylanase leached off to reestablish the dynamic equilibrium between the immobilized enzyme and the solution concentration. Below an equilibrium concentration of ~15 μM, the loading was very much dependent on the solution concentration, but above this, SBA-15 and MSE appeared to be saturated with xylanase at a loading of ~ 4.0 and ~ 6.0 μmol/g respectively. This was in contrast with the adsorption isotherms of cytochrome *c*, where saturation was observed below an equilibrium concentration of ~1−2 μM.

MSE-immobilized cytochrome *c* and MSE- and SBA-15-immobilized xylanase suffer from a significant leaching problem and thus do not form a stable immobilized protein/enzyme. Cytochrome *c* immobilized onto SBA-15 does form a stable immobilized protein. At this point, on the basis of Scheme 1, an alternative support needs to be found for xylanase. Leaching tests, ionic strength studies, and adsorption isotherms all indicate weak interactions with the negatively charged SBA-15 and the more hydrophobic MSE.

Activity Assay. Cytochrome *c* activity was assayed for peroxidative activity using ABTS in the presence of H_2O_2. Previous work by Deere et al.,[11] indicated that immobilized

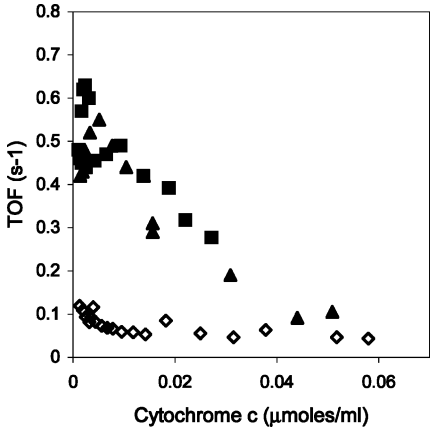

Figure 11. Peroxidative activity of cytochrome *c* (ABTS assay) free and adsorbed onto SBA-15 (2 mg/mL); (■) SBA-15 pH 7, (▲) SBA-15 pH 10, (◇) free cytochrome *c* pH 7.

cytochrome *c* displayed a higher activity than aqueous protein. In that study, cytochrome *c* was immobilized at pH 6.5. In this study, cytochrome *c* was immobilized onto SBA-15 at pH 7 and pH 10 to see if any difference in activity was observed with the different buffers. There was a large enhancement in the turnover frequency (TOF, μmoles of oxidized ABTS produced per second per μmole of cytochrome *c* present) at lower loadings of cytochrome *c* for the adsorbed cytochrome *c* compared to that of the free protein (Figure 11). A similar result was reported by Deere et al.[11] As the loading on SBA-15 approached maximum values of ~30−35 μmol/g in pH 10 buffer and ~20 μmol/g in buffer pH 7, the activity of the adsorbed cytochrome *c* approached that of aqueous cytochrome *c*. Leaching, however, became a problem at these higher loadings. It is likely that at higher loadings, some of the cytochrome *c* molecules are inaccessible to the substrate, and thus, the enhanced activity observed at the lower protein loadings was reduced. Deere et al.[11] reported a similar enhancement in cytochrome *c* peroxidative activity but at much lower loadings. The enhanced activity of cytochrome *c* immobilized onto SBA-15 was maintained up until loadings of ~15 μmol/g, while Deere et al. reported that the activity of the cytochrome *c* immobilized on COS (commercial silicate), MCM-41, CNS (cyano group functionalized silicate), and MPS−F127 with average pore sizes of 55, 130, 28, and 50 Å, respectively, fell to that of aqueous cytochrome *c* at loadings of ~6 μmol/g. This may due to the more spacious pores of SBA-15 compared to those of MCM-41/28, MPS−F127, and COS and the higher surface area and degree of order exhibited (narrower pore size distribution) by SBA-15 compared to those of CNS. The lower surface potential of SBA-15 compared to those materials synthesized with a cationic surfactant may mean that the cytochrome *c* molecules travel further through the pores, resulting in less pore blocking at higher loadings.

Thermostability Studies. The stability of cytochrome *c* to denaturation by heating was studied before and after immobilization onto SBA-15. Figure 12 presents the TOF (turnover frequency) for cytochrome *c*, free and immobilized on SBA-15, that had been incubated at 50 °C and 4 °C for the times indicated prior to peroxidative activity testing at room temperature. Low loadings of cytochrome *c* on SBA-15 were used (3.8 μmol/g), and it was hoped that it would be less susceptible to denaturation in the occluded space of the pores. The immobilization process may result in an opening of the heme cavity, widely reported for cytochrome *c* binding to ionic materials,[31] causing the active heme group to be more accessible

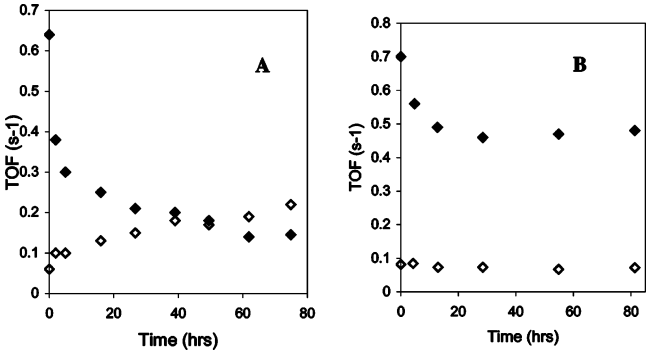

Figure 12. Thermostability of cytochrome *c*, (◇) free (3.1 μM) and (◆) immobilized on SBA-15 (3.8 μmol/g), when incubated at (A) 50 °C and (B) 4 °C.

and therefore resulting in a higher activity. This "opening up" of the protein molecule, however, may make the active site more susceptible to heat denaturation. This would explain the destabilization at 50 °C of cytochrome *c* immobilized onto SBA-15 (Figure 12A) where the activity of the immobilized cytochrome *c* decreased to the value observed for free protein. Free cytochrome *c* (concentration ~3 μM) initially shows an enhancement in activity upon heating, an unexpected result, but this may be a result of initial unfolding of the protein, to allow the active heme site to be more accessible. Incubation at 50 °C for over 3 days resulted in a decrease in the activity of immobilized cytochrome *c* and a small increase in the activity of the free protein. At 4 °C, while the initial enhanced activity of the immobilized cytochrome *c* fell slightly, it still remained much higher than that of free cytochrome *c*. No changes were observed in the room-temperature UV−vis spectrum of cytochrome *c* after incubation at 4 °C and 50 °C for 80 h.

Conclusions

Through the study of the immobilization of cytochrome *c* and xylanase onto the adsorbents SBA-15 and MSE, it has been shown that each of the factors detailed in Scheme 1 as a guide to the generation of an immobilized enzyme are important for the rational design of biocatalysts. The stability of the mesoporous materials at different pH values was checked, and their isoelectric points and zeta potentials were measured. In silico studies of cytochrome *c* and xylanase were conducted before any immobilization experiments in order to select compatible materials and understand the final interactions with the adsorbents. Electrostatic interactions dominated with SBA-15, while weaker hydrophobic interactions may have been the dominant type with MSE for both cytochrome *c* and xylanase. The surface characteristics of xylanase (polar residues) and the weakness of its hydrophobic interactions with MSE suggest a more polar adsorbent might be more successful for its immobilization. The ability of the immobilized protein/enzyme to withstand leaching was measured, and provided it was satisfactory, activity tests and thermostability experiments were conducted. Cytochrome *c* immobilized onto SBA-15 was the only system found to show low leaching. An enhanced activity, compared to that of free protein, was observed. The immobilized cytochrome *c* was shown to have lower thermostability than free cytochrome *c*. High activity and reusability of an immobilized enzyme is the ultimate aim in the rational design of a biocatalyst along with enhanced stability and possible uses as a catalyst in nonaqueous media. Although the successful generation of a biocatalyst was not achieved during this study, this systematic approach, outlined in Scheme 1, to enzyme immobilization is currently being used to develop such biocatalysts.

Acknowledgment. Financial support of this work by Enterprise Ireland (Grant No. SC/2003/0159) is gratefully acknowledged. BASF is thanked for the gift of pluronics. Professor S. Nakahara and Dr. M. Mihov are thanked for the TEM images.

Supporting Information Available: XRD and FTIR data for SBA-15 and MSE; influence of particle size on adsorption and adsorption data concerning the adsorption of xylanase and cytochrome *c* onto SBA-15 and MSE under different experimental conditions. This material is available free of charge via the Internet at http://pubs.acs.org.

References and Notes

(1) (a) Beck, J. S.; Vartuli, J. C.; Roth, W. J.; Leonowicz, M. E.; Kresge, C. T.; Scmitt, K. D.; Chu, C. T.; Olson, D. H.; Sheppard, E. W.; McCullen, S. B.; Higgins, J. B.; Schlenker, J. L. *J. Am. Chem. Soc.* **1992**, *114*, 10834. (b) Kresge, C. T.; Leonowicz, M. E.; Roth, W. J.; Vartuli, J. C.; Beck, J. S. *Nature* **1992**, *359*, 710.

(2) Ryoo, R.; Joo, S. H.; Kim, J. M. *J. Phys. Chem. B* **1999**, *103*, 7435.

(3) Zhao, D.; Huo, Q.; Feng, J.; Chmelka, B. F.; Stucky, G. D. *J. Am. Chem. Soc.* **1998**, *120*, 6024.

(4) Bao, X. Y.; Zhao, X. S.; Li, X.; Chia, P. A.; Li, J. *J. Phys. Chem. B* **2004**, *108*, 4684.

(5) (a) Chong, A. S. M.; Zhao, X. S. *J. Phys. Chem. B* **2003**, *107*, 12650. (b) Asefa, T.; Ozin, G. A.; Grondey, H.; Kruk, M.; Jaroniec, M. *Stud. Surf. Sci. Catal.* **2002**, *141*, 1.

(6) (a) Vinu, A.; Murugesan, V.; Bohlmann, W.; Hartmann, M. *J. Phys. Chem. B* **2004**, *108*, 11496. (b) Antonelli, D. M.; Nakahira, A.; Ying, J. Y. *Inorg. Chem.* **1996**, *35*, 3126.

(7) Feng, X.; Fryxell, G. E.; Wang, L.; Kim, A. Y.; Liu, J.; Kemner, K. M. *Science* **1997**, *276*, 923.

(8) Vinu, A.; Streb, C.; Murugesan, V.; Hartmann, M. *J. Phys. Chem. B* **2003**, *107*, 8297.

(9) Chibata, I. *Immobilised Enzymes*; Hastel Press: New York, 1978.

(10) Diaz, J. F.; Balkus, J. K., Jr. *J. Mol. Catal. B: Enzym.* **1996**, *2*, 115.

(11) Deere, J.; Magner, E.; Wall, J. G.; Hodnett, B. K. *Chem. Commun.* **2001**, 465.

(12) Vinu, A.; Murugesan, V.; Tangermann, O.; Hartmann, M. *Chem. Mater.* **2004**, *16*, 3056.

(13) Vinu, A.; Miyahara, M.; Ariga, K. *J. Phys. Chem. B* **2005**, *109*, 6436.

(14) (a) Yiu, H. H. P.; Wright, P. A.; Botting, N. P. *J. Mol. Catal. B: Enzym.* **2001**, *15*, 81. (b) Yiu, H. H. P.; Wright, P. A.; Botting, N. P. *Microporous Mesoporous Mater.* **2001**, *44*−*45*, 763.

(15) Deere, J.; Magner, E.; Wall, J. G.; Hodnett, B. K. *J. Phys. Chem. B* **2002**, *106*, 7340.

(16) Takahashi, H.; Li, B.; Sasaki, T.; Miyazaki, C.; Kajino, T.; Inagaki, S. *Chem. Mater.* **2000,** *12*, 3301.

(17) Fan, J.; Lei, J.; Wang, L.; Yu, C.; Tu, B.; Zhao, D. *Chem. Commun.* **2003**, 2140.

(18) Sa-Pereira, P.; Paveia, H.; Costa-Ferreira, M.; Aires-Barros, M. R. *Mol. Biotechnol.* **2003**, *24*, 257.

(19) Collins, T.; Meuwis, M.; Stals, I.; Claeyssens, M.; Feller, G.; Gerday, C. *J. Biol. Chem.* **2002**, *277*, 35133.

(20) Brunauer, S.; Emmett, P. H.; Teller, E. *J. Am. Chem. Soc.* **1938**, *60*, 309.

(21) Barrett, E. P.; Joyner, L. G.; Halenda, P. P. *J. Am. Chem. Soc.* **1951**, *73*, 373.

(22) DeLano, W. L. *The PyMOL Molecular Graphics System*; DeLano Scientific: San Carlos, CA, 2002.

(23) Guex, N.; Diemand, A.; Peitsch, M. C. *Trends Biochem. Sci.* **1999**, *24*, 364.

(24) Lehninger, A. L.; Nelson, D. L.; Cox, M. M. *Principles in Biochemistry*, 2nd ed.; Worth Publishers: New York, 1993.

(25) (a) Torronen, A.; Harkki, A.; Rouvinen, J. *EMBO J.* **1994**, *13*, 2493. (b) Torronen, A.; Rouvinen, J.; Ahlgren, M.; Harkki, A.; Visuri, K. *J. Mol. Biol.* **1993**, *233*, 313.

(26) Bao, X. Y.; Zhao, X. S.; Qiao, S. Z.; Bhatia, S. K. *J. Phys. Chem. B* **2004**, *108*, 16441.

(27) Bushnell, G. W.; Louie, G. V.; Brayer, G. V. *J. Mol. Biol.* **1990**, *214*, 585.

(28) Muth, O.; Schellbach, C.; Froba, M. *Chem. Commun.* **2001**, 2032.

(29) O'Reilly, J. P.; Butts, C. P.; I'Anson, I. A.; Shaw, A. M. *J. Am. Chem. Soc.* **2005**, *127*, 1632.

(30) Nicholls, A.; Sharp, K. A.; Honig, B. *Proteins* **1991**, *11*, 281.

(31) (a) Scott, R. A.; Mauk, A. G. *Cytochrome c, A Multidisciplinary Approach*; University Science Books: Sausilito, CA, 1996. (b) Hildebrandt, P.; Heimburg, T.; Marsh, D.; Powell, G. L. *Biochemistry* **1990**, *29*, 1661.